J. Fluid Mech. (2003), *vol.* 482, *pp.* 257–269.
DOI: 10.1017/S0022112003004075 Printed in the United Kingdom

The stability of ducted compound flows and consequences for the geometry of coaxial injectors

By MATTHEW P. JUNIPER AND SEBASTIEN M. CANDEL

EM2C, CNRS, Ecole Centrale Paris, 92295, Châtenay-Malabry, France

(Received 18 March 2002 and in revised form 25 November 2002)

A two-dimensional wake-like compound flow, formed by a low-speed stream embedded within a high-speed flow, is examined in this article. It is shown that the range of absolutely unstable flow in parameter space greatly increases when such a flow is confined within a duct. Parameters studied here are: the density ratio, which is from 0.1 to 1000; the velocity ratio, which varies from co-flow to counter-flow; and the ratio of the duct width to the width of the central jet. Absolutely unstable flows permit perturbations to propagate upstream, and can lead to self-sustained global oscillations similar to the vortex shedding process which takes place in the wake of a bluff body. This theoretical situation models the wake-like behaviour of a two-fluid coaxial injector with a recessed central tube. The aerodynamic destabilizing mechanism is of primary importance whereas the stabilizing mechanisms, which are not considered here, are of secondary importance. The conclusions from this analysis of a ducted compound flow can explain why one observes self-sustained oscillations in recessed coaxial injectors. The presence of a recirculation bubble in the central flow, which is the basis of other proposed explanations, is not required.

1. Introduction

The stability of wake-like compound flows is examined in this article. The model problem features a low-speed stream embedded within a high-speed flow. The effect of enclosing this two-dimensional compound flow within a duct is examined. The analysis is theoretical, although it permits an understanding of experimental observations. The practical situation which motivates this investigation is that of coaxial injectors, which comprise two tubes, one within the other. This configuration is often used to mix a slow dense fluid from the central injector with a fast light fluid from the annular section. The effect of recessing the exit of the central tube within the outer channel is examined here.

It has been known for some time that recessing the central tube of a coaxial injector improves mixing of the two streams; Gill (1978). However, no satisfactory mechanism has yet been proposed. Although the rupture of coaxial jets is complex, an effort is made here to isolate only one feature: the wake-like behaviour of the central flow. This is a severe simplification but the effect of recess can be explained uniquely in terms of this mechanism.

In treating the problem of coaxial injectors, most authors consider only a single shear layer, which means that they cannot model wake-like behaviour. In addition, temporal instability analyses are common, which prevents the modelling of transition to absolute instability. They are also unsuited to this spatial problem. This paper

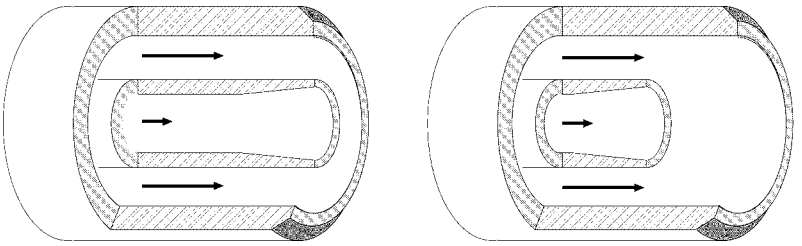

FIGURE 1. Cut-away diagram of a coaxial injector. Left: without recess. Right: with recess.

considers a two-dimensional double shear layer within a duct, with the central stream at low speed. This exhibits wake-like behaviour. A space–time analysis is performed, in order to search for absolute instability. The effect of ducting the compound flow considerably alters its absolutely unstable nature, which has not previously been recognized. This is examined here over density ratios from 0.1 to 1000 and velocity ratios varying from co-flow to counter-flow via a stagnant wake. Four particular values of the ratio of the duct thickness to the thickness of the central flow are examined, from which the behaviour of other values can be inferred. The axisymmetric situation is not covered because the mechanism will be equivalent to the two-dimensional case but mathematically less tractable.

2. Coaxial injectors

2.1. *Description of coaxial injection*

A coaxial injector comprises two cylindrical tubes, one within the other. The tube exits are usually in the same plane but in this article the effect of recessing the central tube is examined. This is shown in figure 1. In many cases a liquid is injected from the central tube and a high-velocity gas is forced through the annular section. This configuration, which is also known as an 'airblast atomizer', Lefebre (1989), can be used to ensure a rapid mixing of the fuels in, for example, a rocket engine. The annular gas stream has a dominant effect when the momentum flux ratio is greater than unity, as shown for example by Lin & Reitz (1998). This is defined as $J \equiv \rho_g U_g^2/\rho_l U_l^2$ and is equivalent to the dynamic head ratio; ρ denotes density, U velocity, subscript g gas and l liquid.

2.2. *Features observed in the fluid flow from a coaxial injector*

The visualizations by Lasheras, Villermaux & Hopfinger (1998) of a liquid jet within a gaseous annular flow show that perturbations develop on the interface between the fluids. These primary instabilities deform into flaps or ligaments which peel off. If the gaseous Weber number, $We_g \equiv \rho_l(U_g - U_l)^2 d_l/\sigma$, is sufficiently high, these are atomized further into droplets. Here, d_l denotes the diameter of the central tube and σ is the surface tension. Although atomization is crucial in practical applications it is not considered here because it is not relevant to the physical mechanism which this article aims to explain. The reader is referred to Lasheras & Hopfinger (2000) for a review.

At moderate We_g, the primary instabilities have a wavelength which is of the order of the central jet diameter. Motion on opposite sides of the jet is coordinated, often in a strong spiral mode. This is fundamentally different from 'pressure atomization', where a single jet discharges into a stagnant gas and the primary instabilities near the injector have a short wavelength: Hoyt & Taylor (1977), Lefebre (1989) and Lin

FIGURE 2. Visualization of the water jet in a laboratory-scale water/air coaxial injector. Water velocity: 0.86 m s^{-1}. Air velocity: 15 m s^{-1}. Radius of water jet: 1.3 mm. Thickness of annulus: 2.7 mm. Top: without recess. Bottom: water exit recessed by 10.3 mm.

& Reitz (1998). This highlights a crucial feature of the coaxial injector, which is that the central fluid behaves like a wake within the annular flow. At high density ratios, wakes are more unstable than jets to long-wavelength perturbations, as shown for example by Yu & Monkewitz (1990).

As the Weber number increases, the characteristic wavelength of perturbations on the central jet decreases by orders of magnitude and coordination from one side of the jet to the other is lost; Lasheras *et al.* (1998). Curiously, however, a long-wavelength helicoidal or sinuous instability occasionally appears, superposed onto the wrinkled central jet, particularly at density ratios between 1 and 100 as indicated by Rehab, Villermaux & Hopfinger (1997) and Juniper (2001). This occurs sporadically when the exit planes of the two injectors are coincident. However, when the central tube is recessed, this long-wavelength mode is sustained permanently. This effect can also be observed at lower velocities on a water/air coaxial injector, as shown in figure 2. Without recess, the central jet is unperturbed. However, when the central jet is recessed, a self-sustained long-wavelength instability appears.

At very high momentum flux ratios ($J > 35$), the central jet is truncated and a recirculating zone exists at its tip, as demonstrated for example by Rehab *et al.* (1997). This is similar to observations of Ko & Lam (1985) and is reminiscent of the wake behind a bluff body with base bleed. This recirculation bubble can also exhibit a helicoidal instability.

2.3. *Mechanisms governing the features observed in coaxial injection*

The flow field in the vicinity of a coaxial injector is shown in figure 3. The two streams are separated by a cylindrical shear layer of thickness δ. Deformation of the interface depends on the balance between destabilizing and stabilizing mechanisms.

The destabilizing mechanism is aerodynamic, as for wind-generated ripples on a free liquid surface. A perturbation at the interface causes the gas to accelerate as it passes a crest, lowering the dynamic pressure at that point. This encourages the crest to increase in size. Perturbations of wavelength λ affect the flow within a radial distance of order λ. Consequently this effect is augmented if the annular flow is confined and has a thickness less than λ, since the gas is increasingly accelerated over the crests.

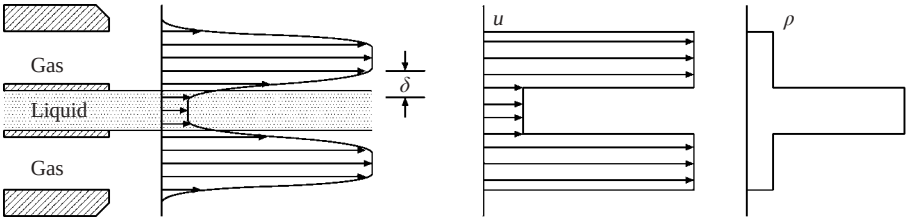

FIGURE 3. Left: sketch of the flow field in the vicinity of a coaxial injector. The shear layer between the gas and liquid has thickness δ. Right: Velocity and density profiles in the inviscid approximation, which is used in this article.

There are two possible stabilizing mechanisms. The fist is surface tension which, if it acts alone, leads to the classical Kelvin–Helmholtz analysis found in Rayleigh (1896, section 365). This model assumes that the shear layer is infinitely thin. The second mechanism can be envisaged by considering the stability of a piecewise shear layer profile, as performed by Rayleigh (1896, section 368). Perturbations of long wavelength compared with the shear layer thickness, δ, are destabilized by the free-stream velocities, via the mechanism described above. However, perturbations which are significantly smaller than δ only experience a constant velocity gradient, which is not inherently destabilizing. In the limit of an infinitely thin shear layer, this situation necessarily tends to the classical Kelvin–Helmholtz analysis without surface tension because the destabilizing mechanism is the same in both cases. This destabilizing mechanism is sometimes thought to be inherent to the inflection point in the velocity profile. This, in fact, amounts to the same mechanism, since any smooth velocity profile between two bulk fluids at different velocities necessarily contains an inflection point. To confirm this, results presented by Esch (1957) demonstrate clearly that the piecewise shear model exhibits the same qualitative behaviour as a realistic shear layer profile.

More advanced models can be created for fluids with different densities, containing both stabilizing mechanisms, as exemplified by Li (1996). In practical situations, which generally correspond to a high Weber number, surface tension only affects wavelengths much smaller than the size of the shear layer and, consequently, does not provide the stabilizing mechanism. The wavelength of the primary instabilities, when not determined by wake-like behaviour, is determined by the thickness of the shear layer. This is confirmed by the experimental studies of Raynal (1997).

Many theoretical studies, such as those by Rehab *et al.* (1997), Lasheras *et al.* (1998) and Villermaux (1998), consider a single two-dimensional shear layer. However, this overlooks a critical aspect of the coaxial injector: its wake-like behaviour. In two dimensions one must consider the interaction of two parallel shear layers, which can generate an absolute instability in the flow, as indicated by Yu & Monkewitz (1990). Absolute instability is necessary, although not sufficient, for the existence of self-sustained global instabilities, as explained further in § 3.1. Furthermore, these authors show that the qualitative behaviour is not affected by the thickness of the individual shear layers. This demonstrates that the wake-like behaviour is inherent to the aerodynamic destabilizing mechanism and interaction of the shear layers. It does not depend qualitatively on the stabilizing mechanism or the thickness of the shear layers.

The dispersion relation of this two-dimensional compound flow is relatively easily derived and solved. An axisymmetric flow is slightly more difficult to handle because it contains modified Bessel functions; Batchelor & Gill (1962). In this article we analyse

only the two-dimensional wake, since Monkewitz (1988*a*) has demonstrated that the axisymmetric case is likely to be qualitatively similar. Another similar situation is that of axisymmetric capillary waves on thin annular liquid sheets, which have been studied by Mehring & Sirignano (2000*a*, *b*), although not for a ducted flow.

The recirculation bubble encountered at high momentum flux ratio exhibits a helicoidal instability reminiscent of a wake flow. This would be predicted by a linear stability analysis similar to that of Monkewitz (1988*a*). An alternative mechanism is proposed by Rehab *et al.* (1997): disturbances in the shear layers are assumed to feed back to the origin of the shear layer via the recirculation bubble, causing self-sustained oscillations. This nonlinear delayed saturation model (NLDS) is applied piecewise in three dimensions in order to consider the axisymmetric case. Its results are consistent with those found by the linear stability analysis but the physics behind the two models is entirely different. Although the NLDS model requires a recirculation bubble, long-wavelength helicoidal instabilities are observed in experiments when a bubble does not exist. This suggests that the NLDS model is not relevant, so only the linear stability analysis is considered in the present article.

2.4. *Comparison of a recessed injector to a ducted wake flow*

In a recessed coaxial injector, the outer stream is contained within a duct, which constrains motion in the radial direction. This is modelled by the velocity and density profiles shown in figure 3. The model has infinite axial extent, which limits its validity because the recessed region has finite length. The absolute instability in globally unstable wakes generally exists only in a small region, usually near its base. This is nevertheless sufficient to trigger a global instability, so the fact that the recessed region is small does not contradict this theory. As a final point, the non-recessed situation would correspond to an unducted wake, where the outer jet is not constrained in the radial direction.

3. The stability of free and ducted compound flows

3.1. *Progression from a convective instability to a global instability*

First it is convenient to review some elements in the analysis of shear flow and wake instabilities. This brief account is based on many recent studies by, for example Yu & Monkewitz (1990), Huerre & Monkewitz (1990), Huerre (2000) and references therein. It is shown by Koch (1985) that a region of local absolute instability exists immediately behind a cylinder in the vortex shedding regime. Mathis, Provansal & Boyer (1984) and Strykowski (1986) demonstrate experimentally that these vortices are shed at low Reynolds number as a result of a global instability. For the Ginzburg–Landau model, the connection between local and global features is analysed further by Chomaz, Huerre & Redekopp (1988) and Huerre & Monkewitz (1990). Monkewitz (1988*b*) shows that the sequence of transitions behind a cylinder wake as the Reynolds number is increased confirms the scenario described by Chomaz *et al.* (1988). This is as follows: transition from stability to convective instability, transition from convective to local absolute instability and finally transition to a self-sustained global mode when a sufficiently large portion of the flow has become absolutely unstable.

Hannemann & Oertel (1989) demonstrate by numerical simulation that only the region directly behind the bluff body is absolutely unstable. This small region may trigger a global mode which influences the entire flow. The behaviour is then similar to a self-excited oscillator. On the theoretical level it is convenient to study the second

step: transition from convective to local absolute instability in a locally parallel flow. This is a necessary (but not sufficient) condition for the existence of a globally unstable mode and it yields useful approximations for the critical parameters leading to global instability.

In a flow behind a cylinder, transition to convective instability takes place at $Re = 5$, according to Monkewitz (1988*b*). The first local absolute instability appears at $Re = 25$, while the experimentally determined onset of vortex shedding occurs around $Re = 45$. Thus in bluff-body wakes, transition to a globally unstable flow occurs for a critical Reynolds number which somewhat exceeds the value corresponding to the appearance of the first local absolute instabilities.

It is indicated by Huerre & Monkewitz (1990) that this approach is supported by the work of Triantafyllou, Triantafyllou & Chryssostomidis (1986). These authors demonstrate that vortex shedding is not caused by flow separation from the bluff-body surface. The experimental results of Inoue (1985) further indicate that vortex shedding disappears when the velocity deficit in the wake is reduced below a critical value. From the last two studies one may deduce that vortex shedding is started by a sinuous global instability in the velocity profile of the wake behind the object and not by the object itself.

The above analyses concern vortex shedding behind a cylinder, which is quasi-two-dimensional. The axisymmetric case behind a bluff body of revolution has also been investigated. Experiments indicate that vortex shedding is helical, at a well-defined Strouhal number. Monkewitz (1988*a*) shows that a region of absolute instability exists just behind the body. These facts are further evidence that a global mode may be responsible for the helicoidal instability, which is similar to the sinuous instability of the two-dimensional wake.

3.2. *Development of a dispersion relation for a two-dimensional ducted compound flow*

A two-dimensional ducted compound flow can simulate the wake-like behaviour of a recessed coaxial injector. The fluids are assumed to be inviscid, with uniform velocity and density. They are bounded above and below by solid walls, as shown in figure 3. These are classical assumptions. In practical applications, injector tubes are several centimetres long and a few millimetres in diameter. Consequently, velocity profiles will be closer to Poiseuille flow initially and then develop into shear layer profiles. However, as indicated by Yu & Monkewitz (1990), these more complex profiles do not change the qualitative behaviour of the double shear layer. For this reason, the classical assumptions are retained. The effect of development of the shear layers is reconsidered in § 3.6.

The outer fluid is denoted by subscript 2 and the central flow by subscript 1. The half-width of the central jet h_1 is used as a reference length. A reference velocity is defined as $u_{ref} = (u_2 + u_1)/2$ and a reference density is ρ_2. This leads to the following non-dimensional variables: $k^* = kh_1$, $c^* = c/u_{ref}$, where $c = \omega/k$, frequency divided by wavenumber. Parameters are the density ratio $S = \rho_1/\rho_2$, the velocity difference $\Lambda = (u_1 - u_2)/(u_1 + u_2)$ and the ratio of annular flow width h_3 to the half-width of the central jet: $h_3^* = h_3/h_1$. If only sinuous and varicose instabilities are considered, the dispersion relation may be cast in the form

$$\Sigma \frac{(1 + \Lambda - c^*)^2}{(1 - \Lambda - c^*)^2} = -1, \tag{3.1}$$

where Σ is the density ratio S weighted by hyperbolic functions of the annular and inner flow thicknesses, relative to the instability wavelength:

$$\Sigma = S\frac{\tanh(k^*)}{\coth(k^*h_3^*)} \quad \text{(sinuous)}, \qquad \Sigma = S\frac{\coth(k^*)}{\coth(k^*h_3^*)} \quad \text{(varicose)}. \tag{3.2}$$

In the case of the unbounded flow, $h_3^* \to \infty$. Consequently, $\coth(k^*h_3^*) \to 1$ and the dispersion relation is identical to that found in Yu & Monkewitz (1990) for unducted compound flows:

$$S\frac{(1+\Lambda-c^*)^2}{(1-\Lambda-c^*)^2} + \coth(k^*) = 0 \quad \text{(sinuous)}. \tag{3.3}$$

This is similar to an unrecessed coaxial injector, where the annular flow is free to expand radially into the ambient fluid.

This model has no stabilizing mechanism, which violates causality for reasons described by Huerre (1987). In practice, this does not cause a problem as long as the analysis is restricted to small wavenumbers, which is the constraint which was identified physically in § 2.3.

3.3. *Geometrical approach to the identification of absolute instability*

The instability characteristics of a flow are most easily demonstrated by considering its response to an impulse, as indicated for example by Huerre & Monkewitz (1990) and Huerre (2000). If the resulting perturbation dies away everywhere, the flow is stable. On the other hand if it is amplified a further distinction is necessary. Convectively stable flows give rise to wave packets which move away from the source and ultimately leave the medium in its undisturbed state. Absolutely unstable flows by contrast are gradually contaminated everywhere by a point-source impulse. This distinction is determined by the contribution of the absolute wavenumber, k_0, defined as the wavenumber with zero group velocity: $\partial\omega/\partial k = 0$. The associated absolute frequency $\omega_0 = \omega(k_0)$ has an absolute growth rate ω_{0i}. If this is negative, the instability is convective. If it is positive, the instability is absolute, subject to fulfilment of the 'pinch' criterion which is defined below.

There is a convenient geometrical approach to this problem. Let $D(\omega, k; P) = 0$ represent the dispersion relation, where P denotes all control parameters. The partial derivatives $\partial\omega/\partial k$ and $\partial D/\partial k$ are related via

$$\left.\frac{\partial\omega}{\partial k}\right|_P \left.\frac{\partial D}{\partial\omega}\right|_{P,k} + \left.\frac{\partial D}{\partial k}\right|_{P,\omega} = 0. \tag{3.4}$$

Thus $\partial\omega/\partial k = 0$ when $\partial D/\partial k = 0$, subject to $\partial D/\partial\omega \neq 0$. The surface $D = 0$ can be traced in the complex k-plane. Saddle points of $D = 0$ in the complex k-plane satisfy $\partial D/\partial k = 0$. Consequently, by equation (3.4), they are points of zero group velocity: (ω_0, k_0). The paths of these saddle points can be followed in (ω, k) space as the control parameters P are varied. By this method, regions of convective instability ($\omega_{0i} < 0$) and absolute instability ($\omega_{0i} > 0$) are determined in parameter space.

There is a further criterion for absolute instability: the regions of unstable flow must propagate into both the $x > 0$ and the $x < 0$ half-planes. This condition can be visualized as the pinching of a k^+ and a k^- branch at a saddle point. The k^+ branch is defined as the path of $D = 0$ in the complex k plane which moves into the $k_i > 0$ half-plane as ω_i is increased. The k^- branch always remains in the $k_i < 0$ half-plane as ω_i is increased. This is the previously mentioned 'pinch' criterion.

A flow that is convectively unstable in one reference plane may become absolutely unstable in another. Consequently, these concepts become relevant only when a reference frame is chosen, which in this case is the exit plane of the central tube.

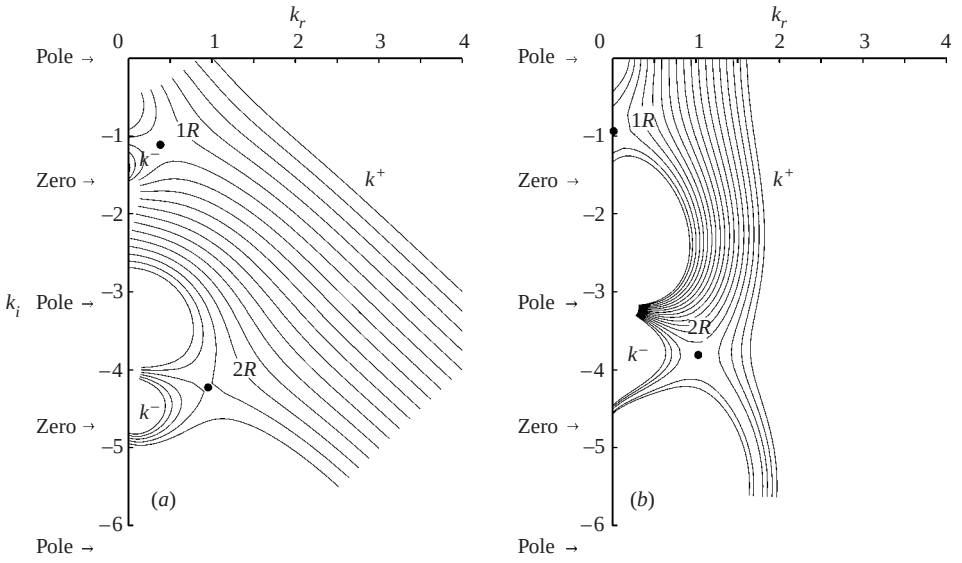

FIGURE 4. Contours of ω_i = constant in the complex k-plane. In both diagrams, the k^+ branch pinches with two k^- branches in this range, forming two saddle points, which are marked •. The dispersion relation is that of the unbounded wake. The velocity parameter, Λ, is equal to -1, corresponding to a static central fluid. (*a*) The density ratio S is equal to 1; (*b*) $S = 830$.

3.4. *Convective/absolute instability transition in a free wake flow*

The geometrical approach is demonstrated in this section for sinuous disturbances of the unducted compound flow, which is somewhat simpler than the ducted compound flow. The dispersion relation is (from this point, the superscript $*$ is dropped from dimensionless variables)

$$D \equiv S\frac{(1+\Lambda-c)^2}{(1-\Lambda-c)^2} + \coth(k) = 0. \tag{3.5}$$

The procedure is similar to that used by Loiseleux, Chomaz & Huerre (1998) where, starting from an approximate solution, saddle points of $D = 0$ are found numerically by solving the nonlinear simultaneous equations $D = 0$ and $\partial D/\partial k = 0$. It is instructive to study an overall map of the dispersion relation (3.5) in the complex k-plane. The function $\coth(k)$ is periodic, repeating in strips of width $\pi\mathrm{i}$ in the k_i-direction. It has simple poles at $k = n\pi\mathrm{i}$ and zeros at $k = (n + 1/2)\pi\mathrm{i}$; $n \in \mathbb{Z}$. These poles and zeros determine the positions of saddle points. Contours of ω_i in the complex k-plane are shown in figure 4(*a*) for a density ratio of 1 and in figure 4(*b*) for a density ratio of 830, which corresponds to water/air at atmospheric pressure. The contours at higher ω_i than the saddle points are k^+ or k^- branches. There is a k^- branch associated with the pole/zero pair in each strip. Since there is a single k^+ branch, one expects an infinite number of k^+/k^- saddle points, one in each strip $n\pi\mathrm{i} > k_i > (n-1)\pi\mathrm{i}$. These saddle points, which scale with h_1, are labelled R, $2R$, $3R$ .... When S is large, a large value of $\coth(k)$ is required for $D = 0$ to be satisfied, which tends to bunch contours around poles. At large S, saddles are closer to poles than they are at small S.

At given parameter values (S, Λ), each saddle point has position (ω_0, k_0). The saddle with the highest value of ω_{0i} causes a local absolute instability if that $\omega_{0i} > 0$.

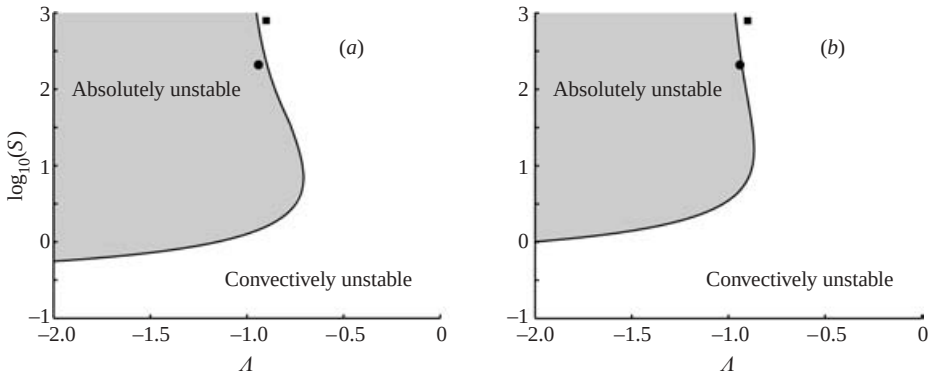

FIGURE 5. Convective/absolute instability transition line for instabilities of an unducted compound flow. Vertical axis: log of the density ratio S. Horizontal axis: non-dimensional velocity ratio, Λ. A co-flow wake is represented by $-1 < \Lambda < 0$. For $\Lambda < -1$ it is counter-flow. The square and circular symbols represent conditions in typical coaxial injectors. (*a*) Sinuous instabilities, (*b*) varicose instabilities. The absolutely unstable domain of sinuous instabilities extends further than that of varicose instabilities.

In this study, saddle points were followed over a wide range of parameter space and the results presented here apply to a wide variety of wake flows. The convective/absolute (CI/AI) transition line can be calculated for each saddle point. Saddle R always has the highest ω_{0i} so only its contribution is shown in figure 5(*a*). This fits exactly the results of Yu & Monkewitz (1990) but is extended here to a higher density ratio. The configuration is more stable in this range, which is not evident in that reference. For comparison, the transition line for the varicose instability is shown in figure 5(*b*).

The operating point of the coaxial injector in a rocket engine is marked by a circle. It lies close to the absolute instability transition line, which suggests that the flow will be marginally globally stable. Huerre & Monkewitz (1990) demonstrate that marginally globally stable flows behave like slightly damped linear oscillators. An impulse can set off an instability very similar to the global mode but it dies away after sufficient time. This behaviour is observed experimentally; Juniper (2001).

3.5. *Convective/absolute instability transition in a ducted wake flow*

For sinuous disturbances in the ducted wake, the $\coth(k)$ term in the disperion relation is replaced by $\coth(k)\coth(kh_3)$. Before tackling this case, it is useful to consider the shape of the dispersion relation with $\coth(k)$ replaced with simply $\coth(kh_3)$. This is shown in figure 6(*a*) for $h_3 = 7$. As before, there is a saddle associated with each k^- branch and there is a k^- branch associated with each pole/zero pair. The poles and zeros are at $n\pi\mathrm{i}/h_3$ and $(n+1/2)\pi\mathrm{i}/h_3$. As expected, the map is qualitatively identical to that for $\coth(k)$ but with the saddles closer together. The saddle points, which scale with h_3, are labelled $1L$, $2L$, $3L$. The CI/AI transition line in (S, Λ) space is identical to that for $\coth(k)$.

When the dispersion relation contains the term $\coth(k)\coth(kh_3)$, there are crucial interactions where poles or zeros associated with $\coth(k)$ are close to those associated with $\coth(kh_3)$. This happens, for example, around the first zero of $\coth(k)$ at $k = -\pi\,\mathrm{i}/2$ and where the two poles coincide at $k = 0$. This is shown in figure 6(*b*).

Let us examine the effect around $k = -\pi\mathrm{i}/2$ first. This concerns the interaction between saddle $3L$ and saddle R. Saddle $3L$ has become more unstable and has a

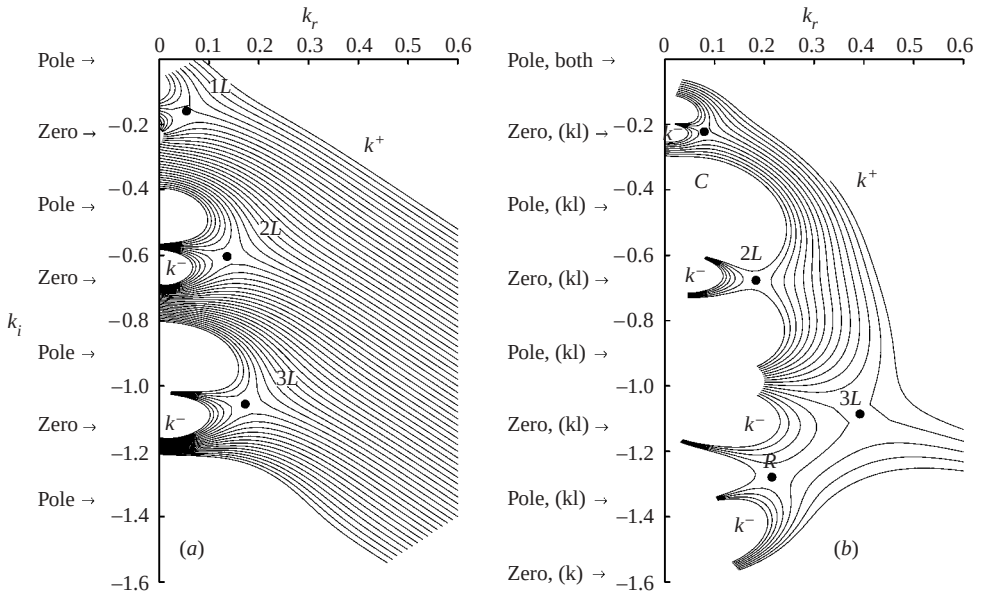

FIGURE 6. Contours of ω_i = constant in the complex k-plane when $S = 1$, $\Lambda = -1$, $h_3 = 7$. In (a), the second term in the dispersion relation (3.5) is $\coth(kh_3)$. The k^+ branch pinches with three k^- branches in this range, forming saddle points $1L$, $2L$ and $3L$, which are marked •. In (b), the second term in the dispersion relation (3.5) is $\coth(k)\coth(kh_3)$, which corresponds to the bounded wake flow. The $1R$ pole of figure 4(a) is now 'superimposed' onto the landscape of (a). The zero of $\coth(k)$ lies close to the third pole of $\coth(kh_3)$, having a strong effect on the contours. With this interaction, saddle $3L$ is more unstable and has a higher wavenumber. It should also be noted that saddle R has become a k^-/k^- saddle point. The saddle point close to the central poles at $k = 0$ is the most affected. This is less visible at $S = 1$ than at $S \gg 1$.

higher ω_{0i} as well as a higher wavenumber. In addition, saddle R has become a k^-/k^- saddle point.

The effect around the pole at $k = 0$ is more significant, although it is less evident at the density ratio of unity shown in figure 6(b). The associated saddle point is denoted C, in order to distinguish it from the L and R family of saddles. Its position changes considerably, particularly at high S, when saddle points approach poles. This effect is most pronounced when $h_3 = 1$, as can be seen from the CI/AI line in (S, Λ) space, figure 7(a). The bounded wake is absolutely unstable over a much wider range of parameter space. This is the key result of this analysis.

Similar effects can be seen for $h_3 = 2.1$ and $h_3 = 7$ in figures 7(b) and 7(c). There is one CI/AI line per saddle point. As h_3 increases, saddle C is unstable over a wide range of velocity ratio but only at high density ratio. The absolutely unstable wavelength that it predicts becomes very large. At lower density ratios, saddle R and the nearby L-saddles are more unstable. As $h_3 \to \infty$, saddle C affects only infinitely high density ratios and all L-saddles collapse to the k_i-axis, where they have zero wavenumber. The family of R-saddles becomes the most unstable as $h_3 \to \infty$ and the behaviour of the unbounded wake is retrieved. The behaviour at $h_3' < 1$ is identical to the behaviour at $h_3 > 1$, where $h_3' \equiv 1/h_3$. It is also worth mentioning that the varicose instability becomes entirely convective as $h_3 \to 1$.

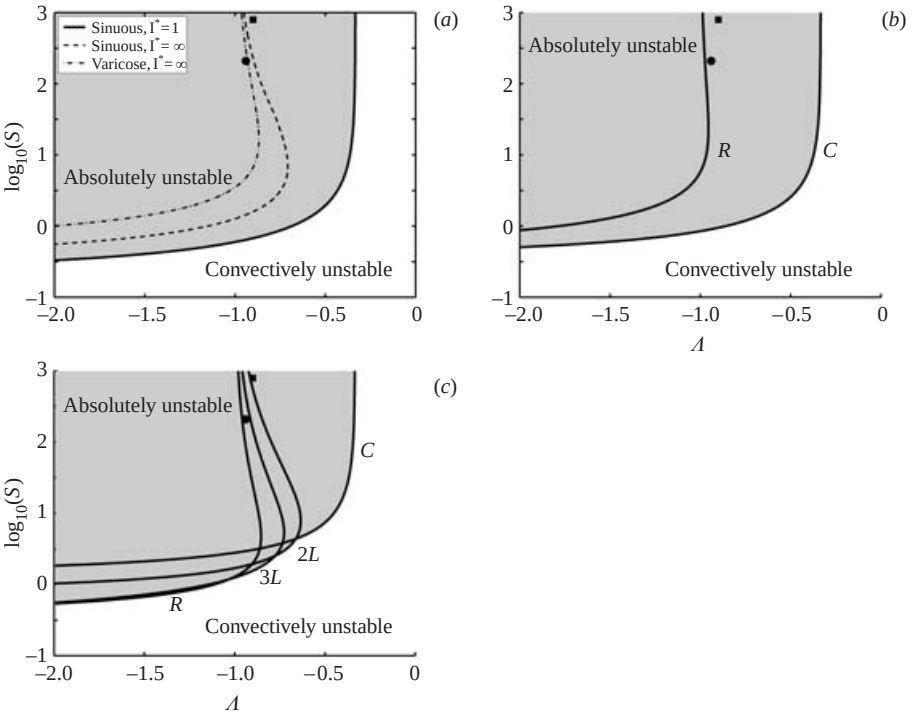

FIGURE 7. Convective/absolute instability transition lines for sinuous instabilities of a ducted compound flow at different values of h_3^*, which is the ratio of the annular width to the inner-flow half-width: (*a*) $h_3^* = 1$, (*b*) 2.1, (*c*) 7. For comparison, the sinuous and varicose transition lines of the unducted flow are shown in (*a*). The letter next to each line in (*b*) and (*c*) denotes the saddle point associated with the line. The square and circular symbols denote typical operating points of coaxial injectors. Ducting the flow causes both operating points to become absolutely unstable to sinuous perturbations.

3.6. *Consequences for the geometry of coaxial injectors*

The model presented here is only valid when the shear layers are infinitely thin. With thicker shear layers the flow has the same qualitative behaviour, Yu & Monkewitz (1990), although the region of absolute instability in parameter space is smaller. In a spatially evolving shear layer, this means that an absolutely unstable region only extends up to a critical shear layer thickness, if it exists at all. Although the critical thickness is not calculated here, it is larger for a ducted compound flow with $h_3 \sim 1$ because sinuous instabilities are absolutely unstable over a larger region of parameter space than for the unducted flow. For the operating point shown as a circle in figures 5 and 7, this suggests that the region of local absolute instability (in physical space) extends much further into the ducted flow than into the unducted flow, as illustrated in figure 8. This would encourage transition to a wake-like global mode, causing self-sustained oscillations.

It is likely that the same effect occurs for an axisymmetric compound flow. The region at the base of the flow is most influential in promoting a global instability. Recessing a coaxial injector is equivalent to ducting this particular region and in practical situations, $h_3 \sim 1$. This suggests that recess lengthens the absolutely unstable region of the flow and therefore encourages transition to a wake-like global mode.

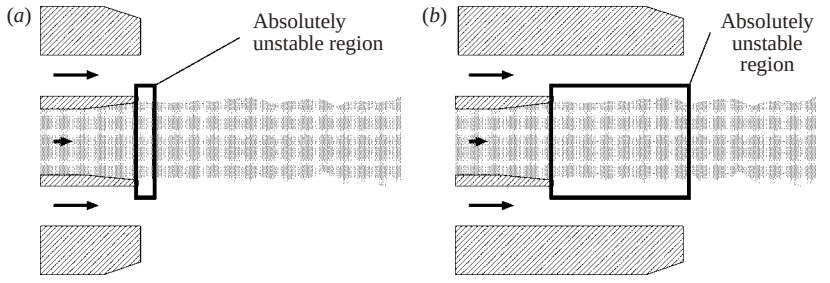

FIGURE 8. Illustrative sketch of regions of absolute instability in a coaxial injector at typical injection conditions. (*a*) Without recess. (*b*) With recess. When the injector is recessed, the larger region of absolute instability is likely to trigger a global mode. This is characterized by self-sustained sinuous or helicoidal oscillations and will cause better mixing of the central jet. Under certain injection conditions an absolutely unstable region might not exist in the non-recessed case.

This is self-sustained and therefore appears permanently, unlike the unrecessed case which is marginally globally stable and where the mode only appears sporadically. The nonlinear development of this flow remains to be determined.

4. Conclusions

It has been observed experimentally that recessing the central tube of a coaxial injector leads to self-sustained wake-like instabilities of the central stream. On the other hand, in an un-recessed injector, these instabilities are only observed intermittently. In this article, a simple model is proposed which contains the necessary physics to simulate the wake-like behaviour of a recessed coaxial injector. It is a two-dimensional wake flow enclosed within a duct. It is shown that this configuration exhibits absolute instability over a much wider range of parameter space than the unducted wake flow. This suggests that the base of a recessed coaxial injector has a much larger absolutely unstable region than that of an unrecessed injector. While the unrecessed injector is marginally globally stable, the recessed injector is globally unstable. This accounts for the experimentally observed behaviour and can aid both the modelling and the design of coaxial injectors in practical applications.

We would like to thank P. Huerre for advice regarding the overall approach, as well as P. Monkewitz and T. Loiseleux for assistance with the geometrical technique. This work has been partially supported by CNES and SNECMA in the framework of the GDR 'Combustion in Liquid Rocket Engines'.

REFERENCES

BATCHELOR, G. & GILL, A. 1962 Analysis of the stability of axisymmetric jets. *J. Fluid Mech.* **14**, 529–551.

CHOMAZ, J., HUERRE, P. & REDEKOPP, L. 1988 Bifurcations to local and global modes in spatially-developing flows. *Phys. Rev. Lett.* **60**, 25–28.

ESCH, R. E. 1957 The instability of a shear layer between two parallel streams. *J. Fluid Mech.* **3**, 289–303.

GILL, G. 1978 A qualitative technique for concentric tube element optimization, utlilizing the factor (dynamic head ratio-1). *AIAA Paper* 78–76.

Hannemann, K. & Oertel, H. 1989 Numerical simulation of the absolutely and convectively unstable wake. *J. Fluid Mech.* **199**, 55–88.

Hoyt, J. & Taylor, J. 1977 Waves on water jets. *J. Fluid Mech.* **83**, 119–127.

Huerre, P. 1987 Spatio-temporal instabilites in closed and open flows. In *Instabilities and Nonequilibrium Structures* (ed. E. Tirapegui & D. Villarroel), pp. 141–177. D. Reidel.

Huerre, P. 2000 Open shear flow instabilities. In *Developments in Fluid Mechanics: A Collection for the Millenium* (ed. G. K. Batchelor, H. K. Moffatt & M. G. Worster). Cambridge University Press.

Huerre, P. & Monkewitz, P. 1990 Local and global instabilities in spatially developing flows. *Annu. Rev. Fluid Mech.* **22**, 473–537.

Inoue, O. 1985 A new approach to flow problems past a porous plate. *AIAA J.* **23**, 1916–1921.

Juniper, M. 2001 Structure et stabilisation des flammes cryotechniques. PhD thesis, Ecole Centrale Paris, Châtenay-Malabry, France.

Ko, N. & Lam, K. 1985 Flow structures of a basic annular jet. *AIAA J.* **23**, 1185–1190.

Koch, W. 1985 Local instability characteristics and frequency determination of self-excited wake flows. *J. Sound Vib.* **99**, 53–83.

Lasheras, J & Hopfinger, E. 2000 Liquid jet instability and atomisation in a coaxial gas stream. *Annu. Rev. Fluid Mech.* **32**, 275.

Lasheras, J., Villermaux, E. & Hopfinger, E. 1998 Break-up and atomization of a round water jet by a high-speed annular air jet. *J. Fluid Mech.* **357**, 351–379.

Lefebvre, A. H. 1989 *Atomization and Sprays.* Hemisphere.

Li, J. 1996 Résolution numérique de l'equation de Navier-Stokes avec reconnection d'interfaces. Méthode de suivi de volume et application à l'atomisation. PhD thesis, Université Pierre et Marie Curie, Paris, France.

Lin, S. & Reitz, R. 1998 Drop and spray formation from a liquid jet. *Annu. Rev. Fluid Mech.* **30**, 85–105.

Loiseleux, T., Chomaz, J. & Huerre, P. 1998 The effect of swirl on jets and wakes: Linear instability of the Rankine vortex with axial flow. *Phys. Fluids* **10**, 1120–1134.

Mathis, C., Provansal, M. & Boyer, L. 1984 The Bénard-von Kármán instability: an experimental study near the threshold. *J. Phys. (Paris) Lett.* **45**, 483–491.

Mehring, C. & Sirignano, W. 2000*a* Axisymmetric capillary waves on thin annular liquid sheets. I. Temporal stability. *Phys Fluids* **12**, 1417–1439.

Mehring, C. & Sirignano, W. 2000*b* Axisymmetric capillary waves on thin annular liquid sheets. II. Spatial Development. *Phys Fluids* **12**, 1440–1460.

Monkewitz, P. 1988*a* A note on vortex shedding from axisymmetric bluff bodies. *J. Fluid Mech.* **192**, 561–575.

Monkewitz, P. 1988*b* The absolute and convective nature of instability in two-dimensional wakes at low Reynolds numbers. *Phys. Fluids* **31**, 999–1006.

Rayleigh, Lord 1896 *The Theory of Sound*, vol. 2. Dover.

Raynal, L. 1997 Instabilité et entrainement à l'interface d'une couche de mélange liquide-gaz. PhD thesis, Université Joseph Fourier, Grenoble I, Grenoble.

Rehab, H., Villermaux, E. & Hopfinger, E. 1997 Flow regimes of large-velocity-ratio coaxial jets. *J. Fluid Mech.* **345**, 357–381.

Strykowski, P. 1986 The control of absolutely and convectively unstable shear flows. PhD thesis, Yale University, New Haven, Connecticut.

Triantafyllou, G., Triantafyllou, M. & Chryssostomidis, C. 1986 On the formation of vortex streets behind stationary cylinders. *J. Fluid Mech.* **170**, 461–477.

Villermaux, E. 1998 Mixing and spray formation in coaxial jets. *J. Propul. Power* **14**, 807–817.

Yu, M.-H. & Monkewitz, P. 1990 The effect of nonuniform density on the absolute instability of two-dimensional inertial jets and wakes. *Phys. Fluids* A **2**, 1175–1181.